

# The Aerodynamical and Structural Analysis of Wind Turbine Blade for Fatigue Prediction

Dr. abbass Z. salman  
 Assistant Prof. University of Technology

## Abstract

The calculation of the dynamic load and stresses acting on wind turbine blades in order to predict fatigue is proposed. In this work the blade element theory was used to calculate aerodynamic loads for small wind turbine blades. This method can also estimate the power extracted by the turbine. A model analysis of rotor was performed using a finite element modeling in order to compute the frequencies and mode shapes. At last, dynamic stresses are computed for the root region of the blades, using finite element modeling. The resulting curves of stress vs. time, obtained for different wind speeds, are used for fatigue analysis in order to make an optimal choice of blades resistant to fatigue and being energetically efficient. In both modal and stress analysis two different approaches are utilized and their results are compared.

## 1. Introduction

Small wind turbine technology can be a meaningful contributor to long-term economic growth by assuring independence in energy supplies and providing benefits to local economy. Moreover wind is a clean non-polluting energy source and the electricity generated by this mean is becoming economically efficient compared to other sources. These blades are exposed to cyclic loading making them vulnerable to cumulative fatigue damage. The prediction of the dynamic behavior of the blades constitutes one of the most important [1].

The prediction of the dynamic behavior of the blades constitutes one of the most important processes in the design of wind turbine [2]. Since it can prevent structural problems such as blade fatigue which is one of the major concerns of designers. Rotor blades are the most flexible part of the wind turbine, and their dynamic behavior has a great influence on the overall performance of the turbine. [3].

Two parts in this work were done the first part include the aerodynamic analysis and in the second part a model analysis is performed by using F.E.M.

## 2. The analysis of The Aerodynamic Behavior.

The objective of this part is to estimate the aerodynamic loads, which are essential to design wind systems. These loads are required for predicting and analyzing wind system energetic performance and for structural design as well [4].

In this aerodynamic modeling two aerodynamic theories are used, the first one is the axial momentum theory and the second is the blade element theory. Because of the complexity of the unsteady flow the use hypotheses are necessary [5]. Also the blade element /momentum formulation blade is necessary to this analysis [6].

### 2.1 The axial momentum theory

In this simple one-dimensional model, airflow is assumed to be incompressible, completely axial and rotationally symmetric.

This model applies the principles of mass and momentum conservation on the annular control volumes surrounding the flow as shown in figure 1.

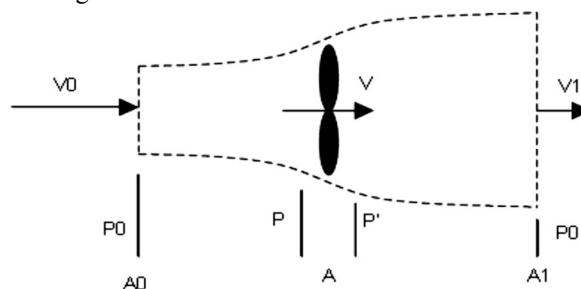


Fig.1 Annular control volume.

Applying the conservation of mass to the control volume yields:

$$V_0 A_0 = V A = V_1 A_1 = V_1 A_1 \quad (1)$$

The thrust force  $T$  at the rotor disc can be found, by applying the conservation of linear momentum to the control

volume in the axial direction[7]:

$$I = m(V_0 - V_1) = \rho A V (V_0 - V_1)$$

Where  $\rho$  is the density of the air.

The thrust is given as:

$$P = \frac{1}{2} \dot{m} (V_0^2 - V_1^2) = \frac{1}{2} \rho A V (V_0^2 - V_1^2) \quad (3)$$

The power extracted from the wind by the rotor is:

$$P = \frac{1}{2} \dot{m} (V_0^2 - V_1^2) = \frac{1}{2} \rho A V (V_0^2 - V_1^2) \quad (4)$$

The power coefficient,  $C_p$ , is defined as the ratio of available power of

$$C_p = \frac{P}{\frac{1}{2} \rho V_0^3 A} \quad (5)$$

Introducing the axial interference factor,  $a$ , which is defined as the fractional decrease in wind velocity between the free stream and the rotor plane:

$$V = (1-a)V_0 \quad (6)$$

The expression of  $C_p$  becomes:

$$C_p = 4a(1-a)^2 \quad (7)$$

### 2.2 The blade element theory:

The control volume used in the previous one-dimensional model can be divided into several annular stream tube control volumes, which split the blade into a number of distinct elements, each of length  $dr$  (fig.2). In this case, the differential area of annular ring at station  $i$ ,  $dA_i$ , is defined as [8]:

$$dA_i = 2\pi r_i dr_i$$

In this theory it is assumed that there is no interference between these blade elements and these blade elements behaviour as airfoils.

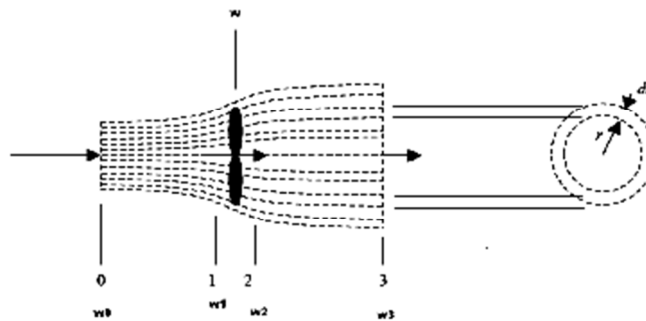


Fig.2 Annular stream tube control volumes

The differential rotor thrust,  $dT$ , at a given span location on the rotor (at a specified  $r$ ) can be derived from the previous theory.

$$dT = 4a(1-a)\rho V_0^2 \pi r dr \quad (8)$$

In order to calculate  $P$  and  $Q$ , the wake angular velocity  $\omega$  has to be known. Introducing, for this purpose, the tangential interference factor  $a'$ , defined as:

$$\omega = a'\Omega \quad (9)$$

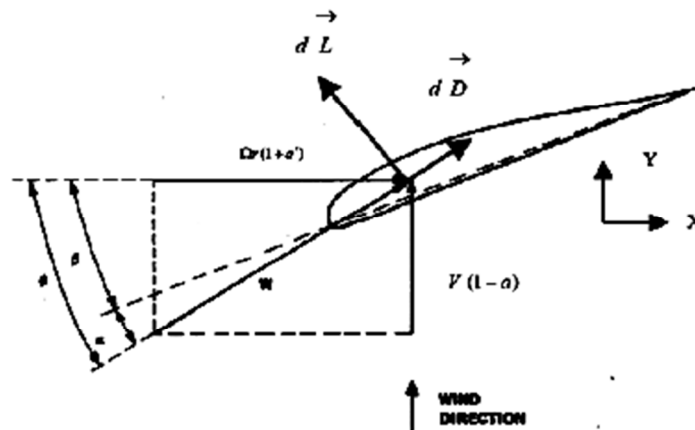


Fig.4 Blade element section at radius  $r$ .

The differential lift and drag forces are:

$$dL = C_L dq \quad (10)$$

$$dD = C_D dq \quad (11)$$

With:

$$dq = \frac{1}{2} \rho W^2 dA = \frac{1}{2} \rho W^2 c dr \quad (12)$$

Where  $C_L$  and  $C_D$  are lift and drag coefficient.

The torque in equations (8), will yield to the expressions of the both interference factors:

$$a = \frac{1}{\frac{4 \sin^2 \phi}{\sigma C_y} + 1} \quad (13)$$

$$a' = \frac{1}{\frac{4 \sin \phi \cos \phi}{\sigma C_x} - 1} \quad (14)$$

Where  $\sigma$  is the local solidity, defined by the following formula:

$$\sigma = \frac{cB}{2\pi r} \quad (15)$$

In order to estimate the load applied on the rotor, an iterative method should be used to determine the values of the interference factor.

For each element at radius  $r$ , the following steps are carried out [9]:

1. An initial reasonable guess of  $a$  and  $a'$  is given.
2.  $C_L$  and  $C_D$  are estimated as a function of  $a$  by approximation method.
3.  $a$  and  $a'$  are finally calculated using equations (13) and (14).
4. These steps are repeated till the successive values of  $a$  and  $a'$  converge.

Once the local (differential) thrust and torque are known they may be integrated numerically, over the length of the blade, to determine the overall torque and thrust as well as the total output power. Table 1 lists the axial and the tangential loads and the torque at different blade stations.

**Table (1) Distribution of aerodynamic loads wind speed 15 m/s profile NACA 63-421**

Station (r/R)	Axial force (N)	Tangential force (N)	Torque (N.m)
0.16	86.02	221.24	206.30
0.25	81.92	351.16	305.56
0.34	73.37	466.19	372.82
0.43	57.87	586.57	467.49
0.51	35.67	764.83	724.62
0.60	39.33	908.37	1120.22
0.69	83.60	998.27	1686.21
0.78	221.50	1012.80	2591.9
0.87	211.31	1109.45	2746.15
0.96	169.79	1181.84	2434.31
1.00	140.04	1206.90	2100.65

The blade motion equation in the flap wise direction can be expressed by the following equation [10]:

$$\frac{\partial^2}{\partial x^2} \left( EI \frac{\partial^2 Z}{\partial x^2} \right) - \frac{\partial}{\partial x} \left( G \frac{\partial Z}{\partial x} \right) + m \frac{\partial^2 Z}{\partial t^2} = \frac{\partial F}{\partial x} \quad (16)$$

Where:

$$G = \int_x^L m \Omega^2 x \, dx, \quad t \text{ is time}$$

$F$  the aerodynamic load.

The mode shapes can be calculated in case of free vibrations (if the blade is not exposed to external loads) using equation (16), which can be written as follows:

$$\frac{\partial^2}{\partial x^2} \left( EI \frac{\partial^2 Z}{\partial x^2} \right) - \frac{\partial}{\partial x} \left( G \frac{\partial Z}{\partial x} \right) + m \frac{\partial^2 Z}{\partial t^2} = 0 \quad (17)$$

By taking  $Z=S(x). (t)$ . And using the method of variable separation, a set of two ordinary differential equations is obtained:

$$\frac{d^2}{dx^2} \left( EI \frac{d^2 S}{dx^2} \right) - \frac{d}{dx} \left( G \frac{dS}{dx} \right) - m \omega^2 S = 0 \quad (18)$$

$$\frac{d^2 \varphi}{dt^2} + \omega^2 \varphi = 0 \quad (19)$$

The boundary conditions of Eq. (18) are:

**At the fixed end of the blade:**

$$\text{Displacement} = 0 \Rightarrow S(0) = 0 \quad (20)$$

$$\text{Slope} = 0 \Rightarrow \frac{dS(0)}{dx} = 0 \quad (21)$$

**At the free end of the blade:**

$$\text{Bending moment} = 0 \Rightarrow \frac{d^2S(L)}{dx^2} = 0 \quad (22)$$

$$\text{Shear force} = 0 \Rightarrow \frac{dS^3(L)}{dx^3} = 0 \quad (23)$$

The rotor used has the following Characteristics

Number of blades: 3

Rotor Diameter: 10 m

Profile: *NACA63-421*

Maximum chord length: 0.6 m

Average chord length: 0.4

The mode shapes obtained, using this approach, are represented by fig. 5 thru 7 and the table (1) is shown the Distribution of aerodynamic loads wind speed 15 m/s profile NACA 63-421.

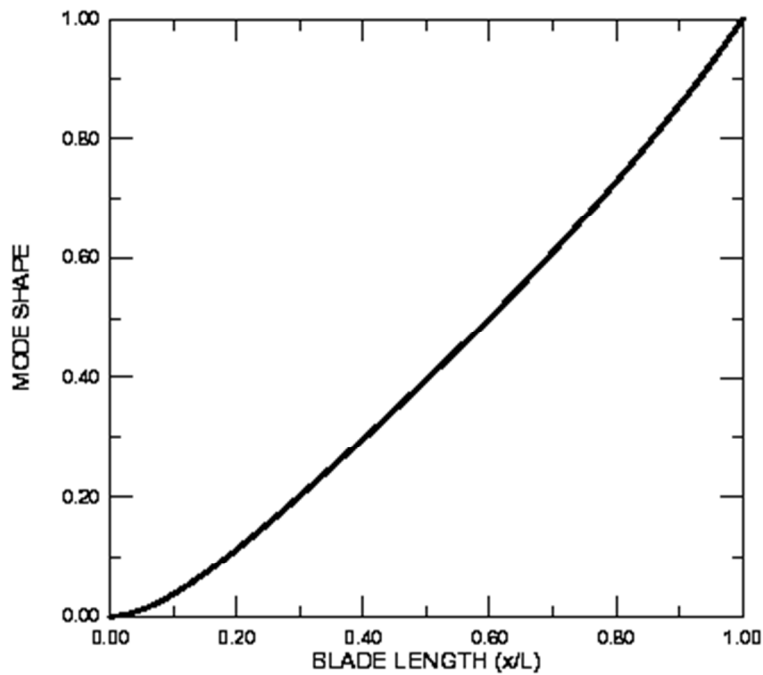


Fig. (1) First flapwise mode shape

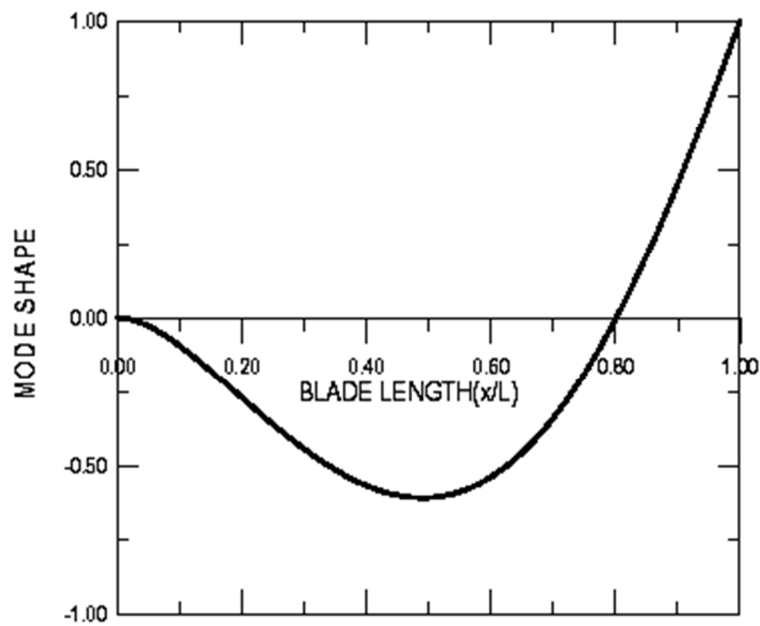


Fig.(2) Second flapwise mode shape

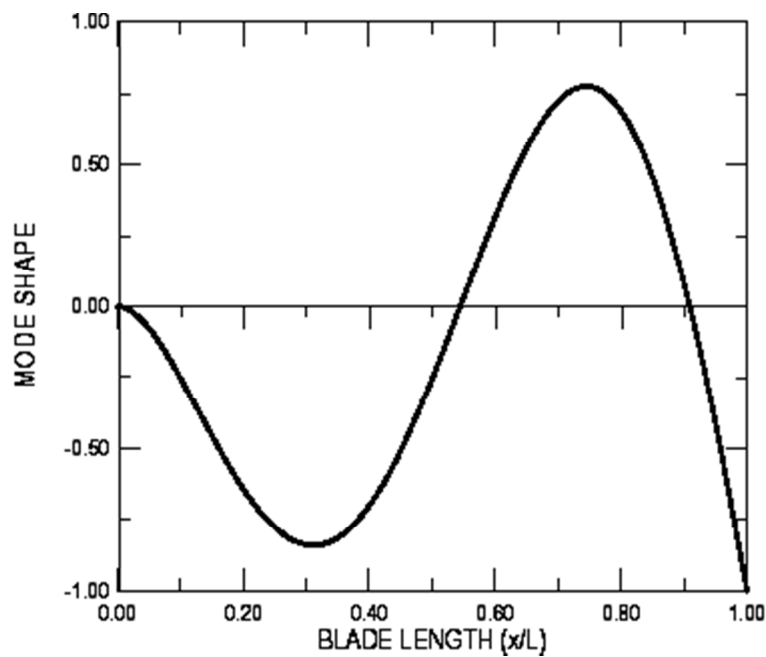


Fig.(3) Third flap wise mode shape

The forced torsional movement is governed by the following equation [10]:

$$\frac{\partial}{\partial x} \left( GJ \frac{\partial \theta}{\partial x} \right) - C \frac{\partial^2 \theta}{\partial t^2} - C \Omega^2 \theta = - \frac{\partial L_A}{\partial x} \quad (24)$$

$C$  the moment of inertia per unit length.

$\Omega$  the angular velocity .

$\theta$  the twist angle .

$L_A$  the aerodynamic moment.

$GJ$  the torsional rigidity .

The solution of this equation is form:

$$\theta = \sum_{i=1}^n Q_i(x) \cdot \phi_i(t) \quad (25)$$

$Q(x)$  the mode shape of torsion.  
 $\varphi(t)$  the response mode.

The free (natural) vibration of the torsional motion can be expressed by the following equation[11]:

$$\frac{\partial}{\partial x} \left( GJ \frac{\partial \theta}{\partial x} \right) - C \frac{\partial^2 \theta}{\partial t^2} - C \Omega^2 \theta = 0 \quad (26)$$

Using similar approach the torsional mode shapes can be obtained, Fig. 8 thru10 represent the torsional mode shapes (Equation (26) can be solved in a similar manner as (18) (bending equation.) :

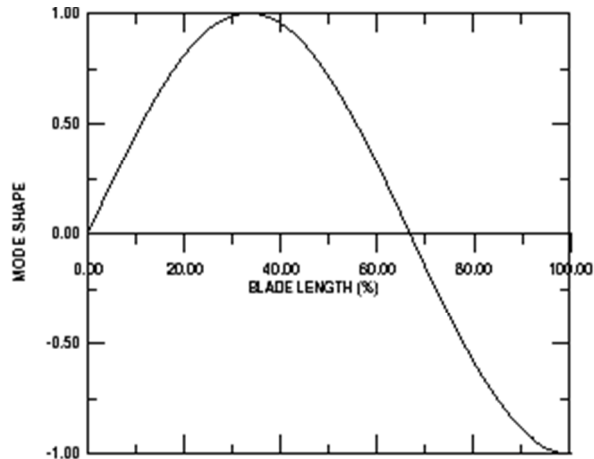


Fig.(4) The second torsional mode shape

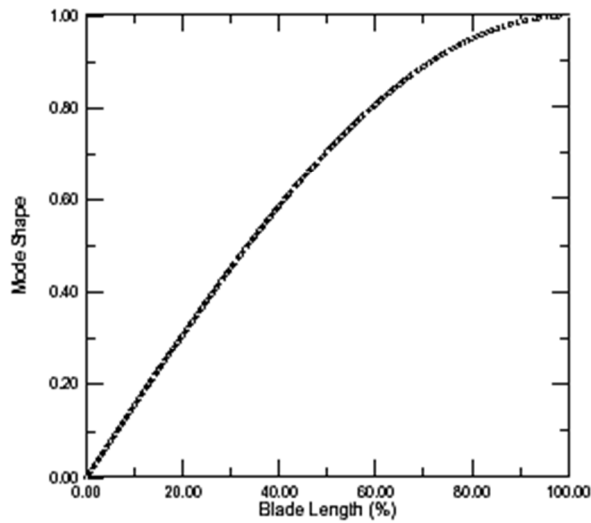


Fig.(5) the first torsional mode shape

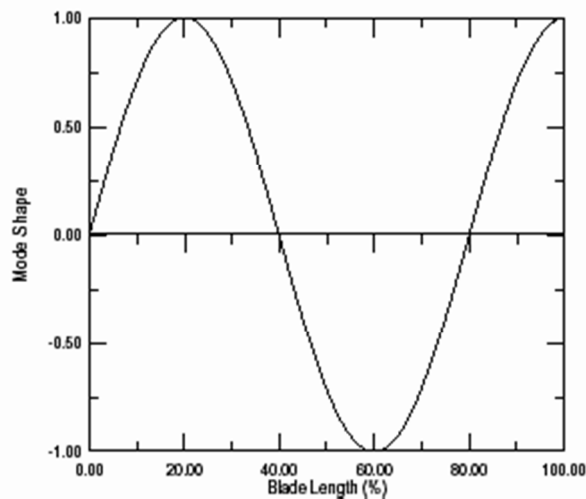


Fig.(6) The Third torsional mode shape.

The mode shapes verify the property of orthogonally defined as follows [10]:

$$\int_0^L Q_i(x)Q_j(x)dx = 0 \quad \text{if } i \neq j$$

$$\int_0^L Q_i(x)Q_j(x)dx = f(i) \quad \text{if } i=j$$

If this solution (25) is substituted in the equation(24) and by taking account of the mode orthogonally, one obtains:

$$\frac{d^2\phi_i(t)}{dt^2} + \omega_i^2\phi_i(t) = \frac{1}{C f(i)} \int_0^L \frac{\partial L_A}{\partial x} Q_i(x) dx \quad (27)$$

The method of solving equation (27) is similar to that of equation (24).

### 3. Calculation of the dynamic stress to prediction fatigue failure by using F.E.M:

The method used in this part is a finite element modeling of a real blade with complex geometry [12]. This blade is twisted, with a variable chord length and having a complex shape at the root region.

The rotor used has the following Characteristics

Number of blades: 3

Rotor Diameter: 10 m

Profile: *NACA63-421*

Maximum chord length: 0.6 m

Average chord length: 0.4

Maximum twist angle: 14°

After the geometrical modelling and meshing of this blade, the following figure is obtained (fig.7):

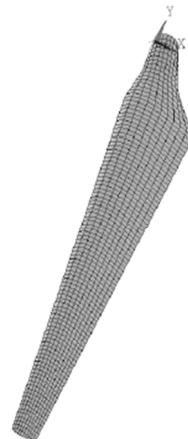


Fig.(7) Geometry modeling of the blade

### 3.1 mode shapes and Calculation of the frequencies of the blades

The modal analysis of the rotor is carried out giving the following results:

Table 2 gives the first three bending frequencies.

Table 2 blade natural frequencies

Mode number	Frequency $\omega$ (Hz) (Motion Eq)	Frequency $\omega$ (Hz) (FEM)
First mode	9.40	8.37
Second mode	15.81	14.94
Third mode	57.36	62.74

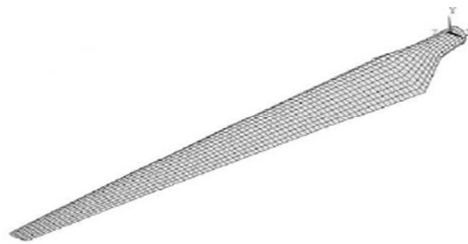


Fig.(8) First mode shape deformation

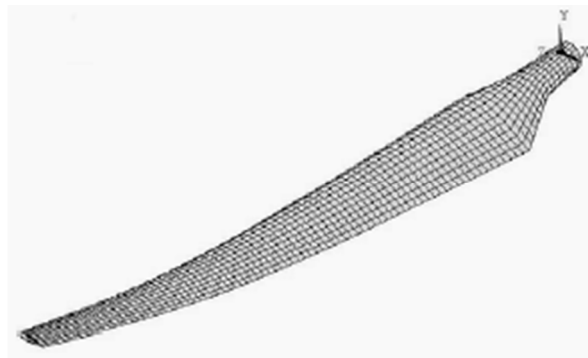


Fig.(9) Second mode shape deformation

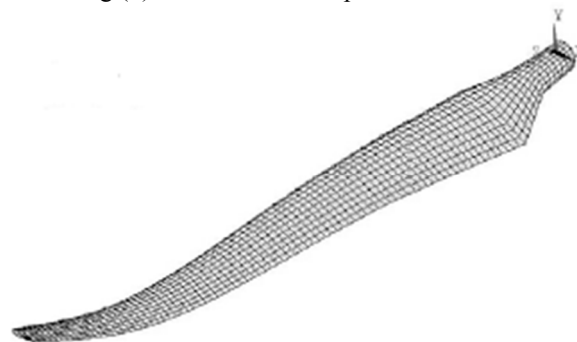


Fig.(10)Third mode shape deformation

The flap wise mode shape curves are given by fig.(11) thru (13).

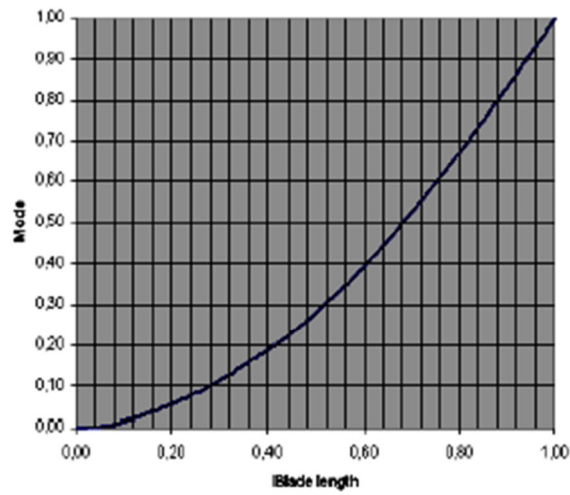


Fig.(11) First flap wise mode shape

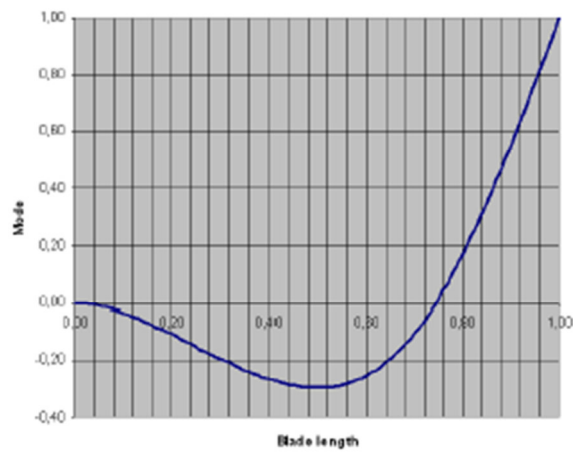


Fig.(12) Second flapwise mode shape

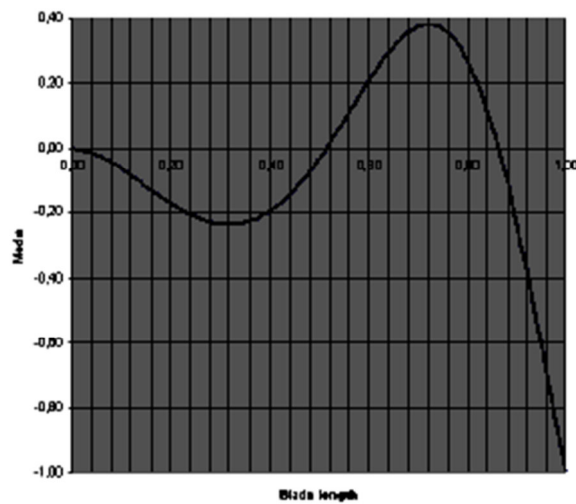


Fig.(13) Third flapwise mode shape

A dynamic analysis of the rotor using finite element modelling is carried out. The following results of the dynamic stresses, at the root region of the blade, are obtained for different wind speeds (fig.14 thru fig.20):

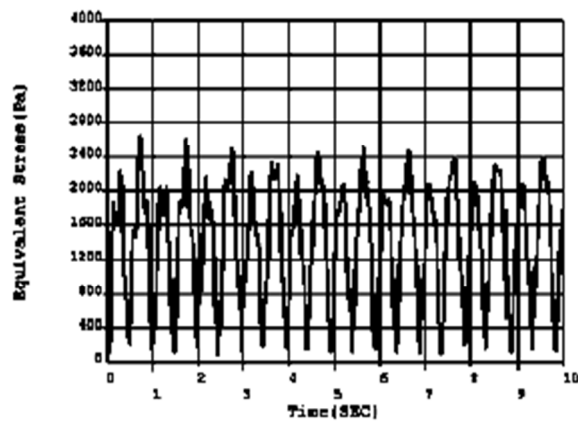


Fig.(14) Equivalent alternating stress at the blade root  
Profile *NACA63-421* Material composite  
(wind speed 4 m/s)

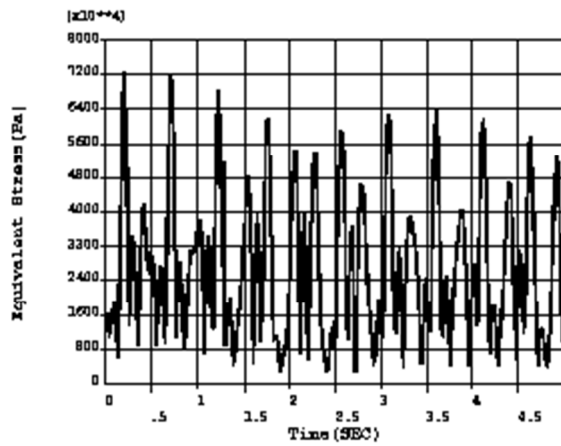


Fig.(15) Equivalent alternating stress at the blade root  
Profile *NACA63-421* Material composite  
(wind speed 15 m/s)

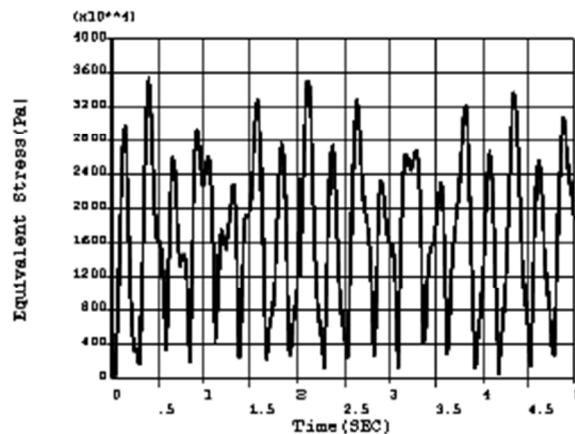


Fig.(16) Equivalent alternating stress at the blade root  
Profile *S809* Material composite  
(wind speed 7 m/s)

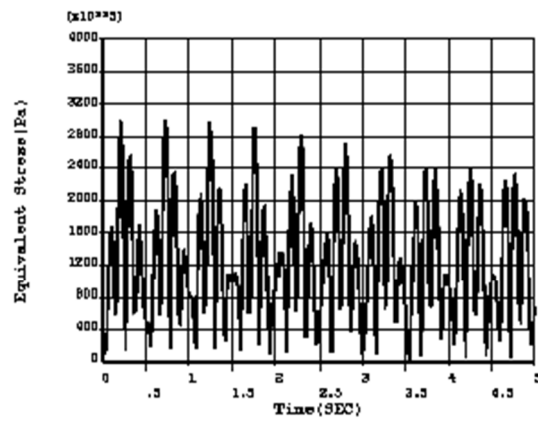


Fig.(17) Equivalent alternating stress at the blade root Profile *S809* Material composite (wind speed 15 m/s).

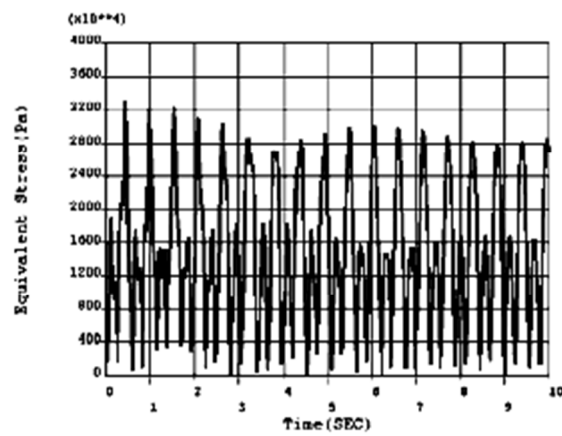


Fig.(18) Equivalent alternating stress at the blade root Profile *NACA63-421* Material Aluminum (wind speed 7 m/s)

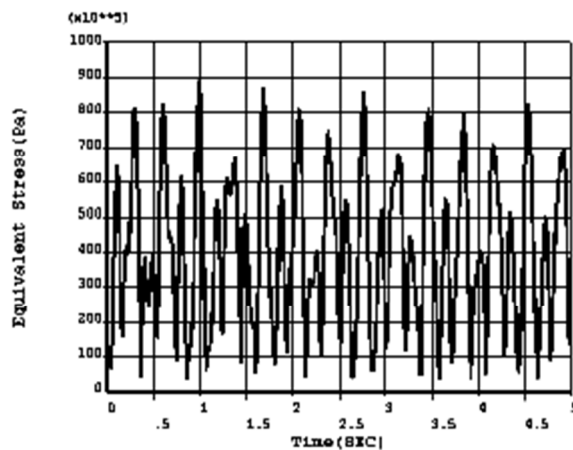


Fig.(19) Equivalent alternating stress at the blade root Profile *NACA63-421* Material Aluminum (wind speed 11 m/s)

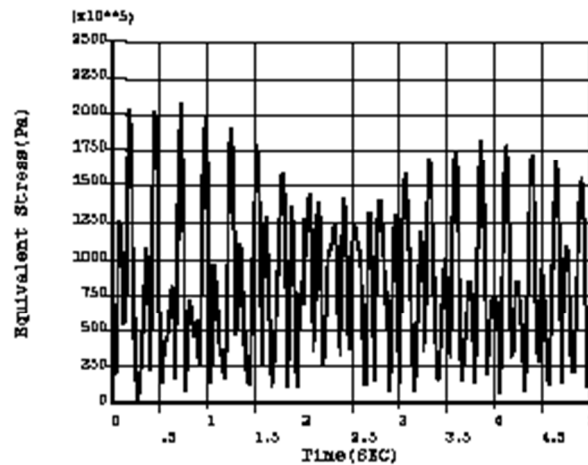


Fig.(20) Equivalent alternating stress at the blade root Profile *NACA63-421* Material Aluminum (wind speed 15 m/s)

#### 4. Blade Fatigue Calculation.

The fatigue of the blades is estimated based on Miner theory, which can be applied in the case of a machine part operating under alternative stress having variable amplitude. This theory is known as «the linear cumulative damage rule » or « Miner’s rule. » It assumes that every operating cycle consumes a percentage of the part life. Hence the total wear of the part can be estimated by adding up the percentage of life consumption by each overstress cycle. Miner theory is stated mathematically as follows [13]:

If stresses with amplitudes  $\sigma_1, \sigma_2, \dots, \sigma_k$  are applied to a machine part for a total number of cycles  $n_1, n_2, \dots, n_k$  respectively and if the lives (the allowable number of cycles) corresponding to (the allowable number of cycles) corresponding to these stresses are :  $N_1, N_2, \dots, N_k$  then failure may occur if :

$$\frac{n_1}{N_1} + \frac{n_2}{N_2} + \dots + \frac{n_k}{N_k} = 1 \quad (28)$$

Miner cites numerous tests that showed if the loading were random, equation (28) would usually

give conservative predictions (i.e.  $\sum_i \frac{n_i}{N_i} > 1$ )

In this work a three-blade wind turbine is used with a NACA profile. The values of  $n_i$  are calculated for the lifetime period from the statistical distribution of wind speed (fig.18), while the values of  $N_i$  are taken from the endurance limit curve [14].

##### 4.1 Fatigue calculation of aluminum alloy blades

In the case of aluminum alloy blades, the operating life time is assumed to be ten years.

The probability so that the speed of the wind is included in a given interval is estimated using the curve of fig.18. This data is used in the calculation of the number of cycles  $n_i$  completed, under this speed, during ten year of operation. The amplitude of the stress is estimated from the curve of dynamic stresses, corresponding to this speed. Finally the allowable number of cycles  $N_i$  (lifetime) is determined from the fatigue strength curve.

As example, the probability so that the speed of the wind is in the velocity of 7 m/s ( $6 \leq V \leq 8$ ) is 0.05, in this case the number of cycles carried out is:

$$n_i = \frac{0.05 \times 3600 \times 24 \times 365 \times 10^4 \times V \cdot \lambda}{2\pi R} = 2.4 \times 10^7$$

This calculation is repeated for different speed ranges. The results of this calculation are given in table 3. The wear ratio is estimated by the formula (28) as follows:

$$\sum_i \frac{n_i}{N_i} = \frac{7.6 \times 10^6}{5 \times 10^7} + \frac{4.1 \times 10^5}{5 \times 10^5} = 0.972$$

According to the rule of miner these blades can resist fatigue for ten years of operation, since the ratio

$\sum_i \frac{n_i}{N_i}$  is lower than 1.

#### 4.2 Fatigue calculation of composite material blades

In the same manner, it's deduced that blades of composite material and having the same profile can resist fatigue for twenty years of operation. The results of this calculation are given in table 4.

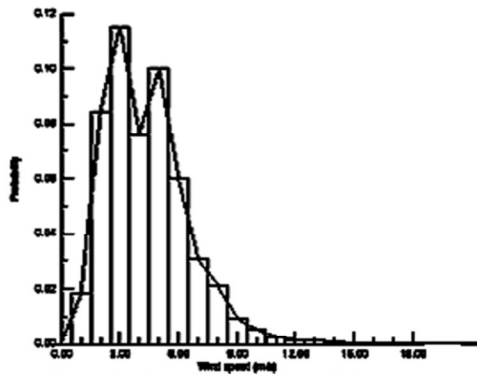


Fig.21 Statistical distribution of wind speed

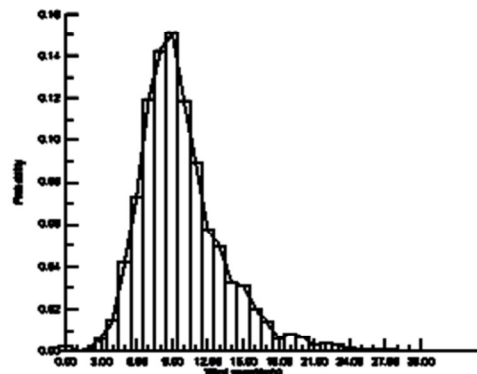


Fig.22 Statistical distribution of maximum wind

Table 3 Fatigue calculation (aluminium alloy blades)

Wind Speed (m/s)	4	7	11	15
Stress amplitude (Mpa)	10	30	80	175
$n_i$ (cycles of operation)	$4.7 \times 10^7$	$2.4 \times 10^7$	$7.6 \times 10^6$	$4.1 \times 10^5$
Life $N_i$ (cycle)	infinite	infinite	$5 \times 10^7$	$5 \times 10^5$

Table 4 Fatigue calculation (composite material blades)

Speed of wind (m/s)	4	7	11	15
Stress Amplitude (Mpa)	24	30	40	64
$n_i$ (cycles of operation)	$9.4 \times 10^7$	$4.8 \times 10^7$	$1.5 \times 10^6$	$8.2 \times 10^5$
Life $N_i$ (cycle)	infinite	infinite	$10^{10}$	$10^8$

#### 5. Conclusions

In this work the blade element theory was used to calculate aerodynamic loads for small wind turbine blades. This method can also estimate the power extracted by the turbine. A modal analysis of rotor was performed using a finite element modeling in order to compute the frequencies and the mode shapes of the blades. The modal analysis was also carried out in a different way using the blade motion equation. The result of finite element modeling agrees well with that obtained by the other approach, since the corresponding frequencies have close values and the mode shapes are similar.

The resulting mode shapes were also compared with those obtained by Baumgart [15], the corresponding modes have similar shapes. At last, dynamic stresses were calculated for the root region of the blades using finite element modeling. This region is a highly loaded and structurally complex area. These obtained dynamic stresses were used to estimate the blade fatigue, in order to make an optimal design of blades that resist fatigue and being energetically efficient.

The fatigue calculation has shown, according to Miner rule, that a rotor made of composite material and having a NACA63-421 profile can withstand fatigue failure for duration close to 20 years with an operating speed exceeding 15 m/s.

In order to make conservative estimation of fatigue, one can use the statistical distribution of maximum wind speed (fig. 21). The interdependence between the aerodynamic load and the blade deflection known as Aeroelastic phenomenon, is the most challenging problems in the design of wind turbines since it causes a great deal of computational complexity. The minimum cost of energy is the criterion actually used to optimize blade geometry rather than maximum annual energy production. The optimization of wind turbine based on Minimum cost of energy requires a multidisciplinary method that includes aerodynamic and structural models for blades along with a cost model for the whole turbine [16]. This work can be a part of a global optimization study aiming

to minimize cost and structural problems of wind turbine while maximizing its energetic performance.

### References

- [1] P.S. Veers, T.D. Ashwill, Trends in Design Manufacture and Evaluation of Wind Turbine, Wind Energy, Vol.6, 2003, pp. 245-259.
- [2] K.O. Ronoldk, Reliability-based Fatigue Design of Wind Turbine Rotor Blades, Engineering Structures, Vol.21, 1999, pp. 1101-1114.
- [3] Abbass Z. Salman, Roshen T. Ahmed. "The comparison analysis of fixed pitch angle wind turbine generator ", National Renewable Energies Conference and Their Applications/ University of Technology, 2013
- [4] P.S Veers, T.D. Ashwill, Trends in Design Manufacture and Evaluation of Wind Turbine, Wind Energy, Vol.6, 2003, pp.245-259.
- [5] W. Can-Xing, S. Xi, Numerical Simulation of Three Dimensional Flow in a Centrifugal Fan, WSEAS Transactions on Applied and Theoretical Mechanics, Vol.1, No.1, 2006.
- [6] Abbas z . Salman "Flutter Phenomena Effected By Aerodynamic Load "Engineering &Technology Journal .University of Technology, 2005,No.3 vol.24.
- [7] E. Lysen, Introduction to Wind Energy, Netherlands: Amersfort, 2nd
- [8] J.M. Jonkman, Modeling of the UAE Wind Turbine for Refinement of Fast Ad, National Renewable Energy Laboratory, Task No. WER3 2010 NREL/TP-500-34755, December 2003.
- [9] D. Wood, Design and Analysis of Small Wind Turbine, New castle Australia, University of New Castle, 2002.
- [10] A. Bramwell, Helicopter dynamic, Edward Arnold, New York, 1989.
- [11] Z.L, Mahri, M.S, Rouabah, Aeroelastic Simulation of a Rotating Wind Turbine Blade, International Conference on Fluid Mechanics, WSEAS Press, Mexico, 2008.
- [12] L. Vasiliauskiene, S. Valentinavicius, A. Sapalas, Adaptive Finite Element Analysis for Solution of Complex Engineering Problems, WSEAS Transactions on Applied and Theoretical Mechanics, Vol.1, No.1, 2006.
- [13] M. Nielsen, G.C. Larsen, J. Mann, Wind Simulation for Extreme and Fatigue Load, Riso Laboratory, Riso-R-1437(EN), 2004.
- [14] H. Teodorescu, S. Vlase, D. Nicoara, Mechanical Behaviour of pre-Tensioned Glass Fiber Reinforced Composite Tubes Subjected to Internal Pressure, WSEAS Transactions on Applied and Theoretical Mechanics, Vol.2, No.2, 2007.
- [15] A. Baumgart, a Mathematical Model for Wind Turbine Blade, Journal of Sound and Vibration, Vol.251, 2002, pp. 1-12.
- [16] J.L. Tangler, The Evolution of Rotor and blade Design, American Wind Energy Conference, 2000.